

## ORIGINAL ARTICLE

# IL-21 treatment recovers follicular helper T cells and neutralizing antibody production in respiratory syncytial virus infection

Rodrigo Benedetti Gassen<sup>1,2,3</sup>, Tiago Fazolo<sup>1,2</sup>, Deise Nascimento de Freitas<sup>2</sup>, Thiago J Borges<sup>3</sup>, Karina Lima<sup>1,4</sup>, Géssica L. Antunes<sup>2</sup>, Fábio Maito<sup>5</sup>, Daniel AG Bueno Mendes<sup>6</sup>, André Báfica<sup>6</sup>, Luiz Carlos Rodrigues Jr<sup>7</sup>, Renato Stein<sup>8</sup>, Ana Paula Duarte de Souza<sup>2</sup> & Cristina Bonorino<sup>4,9</sup>

- 1 Laboratório de Imunologia Celular e Molecular, Pontifícia Universidade Católica do Rio Grande do Sul, Porto Alegre, Brazil
- 2 Laboratório de Imunologia Clínica e Experimental, Pontifícia Universidade Católica do Rio Grande do Sul, Porto Alegre, Brazil
- 3 Renal Division, Schuster Family Transplantation Research Center, Brigham and Women's Hospital, Harvard Medical School, Boston, MA, USA
- 4 Laboratório de Imunoterapia, Universidade Federal de Ciências da Saúde de Porto Alegre, Porto Alegre, Brazil
- 5 Laboratório de Histologia, Faculdade de Odontologia, Pontifícia Universidade Católica do Rio Grande do Sul, Porto Alegre, Brazil
- 6 Laboratório de Imunobiologia, Universidade Federal de Santa Catarina, Florianópolis, Santa Catarina, Brazil
- 7 Laboratório de Imunovirologia, Universidade Federal de Ciências da Saúde de Porto Alegre, Porto Alegre, Brazil
- 8 Infant Center, Pontifícia Universidade Católica do Rio Grande do Sul, Porto Alegre, Brazil
- 9 Department of Surgery, School of Medicine, University of California at San Diego, La Jolla, CA, USA

## Keywords

Follicular helper T cells, IL-21, IL-21R, PD-L1 blockade, respiratory syncytial virus

## Correspondence

Rodrigo Benedetti Gassen, Laboratório de Imunologia Celular e Molecular, Pontifícia Universidade Católica do Rio Grande do Sul, Brazil.

E-mail: [rbgassen@gmail.com](mailto:rbgassen@gmail.com)

Received 3 July 2019;

Revised 31 July and 8 October 2020;

Accepted 14 October 2020

doi: 10.1111/imcb.12418

*Immunology & Cell Biology* 2021; **99**: 309–322

## Abstract

Respiratory syncytial virus (RSV) is the major cause of lower respiratory tract infections in children under 1 year. RSV vaccines are currently unavailable, and children suffering from multiple reinfections by the same viral strain fail to develop protective responses. Although RSV-specific antibodies can be detected upon infection, these have limited neutralizing capacity. Follicular helper T (T<sub>fh</sub>) cells are specialized in providing signals to B cells and help the production and affinity maturation of antibodies, mainly via interleukin (IL)-21 secretion. In this study, we evaluated whether RSV could inhibit T<sub>fh</sub> responses. We observed that T<sub>fh</sub> cells fail to upregulate IL-21 production upon RSV infection. In the lungs, RSV infection downregulated the expression of IL-21/interleukin-21 receptor (IL-21R) in T<sub>fh</sub> cells and upregulated programmed death-ligand 1 (PD-L1) expression in dendritic cells (DCs) and B cells. PD-L1 blockade during infection recovered IL-21R expression in T<sub>fh</sub> cells and increased the secretion of IL-21 in a DC-dependent manner. IL-21 treatment decreased RSV viral load and lung inflammation, inducing the formation of tertiary lymphoid organs in the lung. It also decreased regulatory follicular T cells, and increased T<sub>fh</sub> cells, B cells, antibody avidity and neutralization capacity, leading to an overall improved anti-RSV humoral response in infected mice. Passive immunization with purified immunoglobulin G from IL-21-treated RSV-infected mice protected against RSV infection. Our results unveil a pathway by which RSV affects T<sub>fh</sub> cells by increasing PD-L1 expression on antigen-presenting cells, highlighting the importance of an IL-21–PD-L1 axis for the generation of protective responses to RSV infection.

## INTRODUCTION

Respiratory syncytial virus (RSV) is the leading cause of lower respiratory tract infection in infants, responsible for about 3 million hospitalizations and 74 500 deaths

worldwide every year in children under 5 years of age.<sup>1</sup> There is no effective vaccine available against RSV, and passive immunization with monoclonal antibodies is used only in high-risk infants. Pregnant women and the elderly

are also target populations,<sup>2</sup> reinforcing the need for the development of an effective vaccine.

In humans, neutralizing RSV-specific antibodies are formed in the upper respiratory tract. However, reinfection with the same RSV strain is frequent in immunocompetent individuals, because antibody responses rapidly decline (approximately 3 months) to preinfection levels, which may facilitate recurring infections.<sup>3,4</sup> A correlation between nasal pre-existing RSV-specific humoral response and resistance to reinfection has been reported.<sup>5</sup> Other studies have correlated the presence of serum high-avidity RSV-specific immunoglobulin (Ig)G with protection,<sup>6</sup> although these antibodies have a short half-life in children<sup>7</sup> and adults.<sup>8</sup> RSV morbidity and mortality are increased in 2–4-month infants, in whom titers of maternal antibodies are reduced and have not yet been replaced by an endogenous antibody response.<sup>9</sup> The RSV fusion (F) protein is a glycoprotein on the envelope of the virion and the main target of antibodies leading to RSV neutralization; however, only a poor neutralizing antibody response is induced by the postfusion form of the RSV F protein. Antibodies that target the F pre-fusion form appear to be more effective as a neutralizing response.<sup>10,11</sup>

Effective B-cell responses require help from follicular helper T (Tfh) cells, which are found predominantly in germinal centers (GCs) of secondary lymphoid organs.<sup>12–14</sup> Tfh cells constitute the main source of interleukin (IL)-21.<sup>15</sup> IL-21 binds to interleukin-21 receptor (IL-21R) in naïve B cells and, along with other costimulatory signals, drives differentiation of either memory, GC B cells or plasma cells.<sup>16</sup> IL-21 is also crucial for affinity maturation and class switching of antibodies<sup>17</sup> that protect against invading pathogens.<sup>18,19</sup> Tfh cell activity can be negatively regulated by regulatory follicular T cells (Tfr cells), which are Foxp3-expressing follicular T cells with a regulatory phenotype.<sup>20</sup> Tfh cell regulation by Tfr cells involves different suppressor mechanisms, including downregulation of B-cell stimulation, delivery of direct negative signals and secretion of suppressive cytokines.<sup>21</sup>

In this study, we hypothesized that RSV targets humoral immune response efficiency by negatively modulating Tfh cells, thus preventing B-cell help. Our results showed that, upon RSV infection, Tfh cells failed to produce IL-21 and downregulated IL-21R. This correlated with a low-avidity RSV-specific humoral immune response, viral proliferation and lung tissue damage. GC response, which is stimulated by IL-21, is decreased by RSV infection, but can be recovered by treatment with recombinant IL-21. Treatment also induced the formation of tertiary lymphoid organs

(TLOs) in the lung, reduced Tfr cells both in lung draining lymph nodes (LDLNs) and in lungs and restored high-affinity antibody production, decreasing viral replication and viral-induced lung inflammation. RSV infection also led to expression of programmed death-ligand 1 (PD-L1) in dendritic cells (DCs) and B cells, which correlates with decreased B- and Tfh-cell function. Blockade with anti-PD-L1 recovered IL-21R expression in Tfh cells and restored the secretion of IL-21 in a DC-dependent manner. Our results showed an intricate cooperation between the programmed cell death protein 1 (PD-1)/PD-L1 and the IL-21/IL-21R pathways in the generation of effective anti-RSV protective antibody responses.

## RESULTS

### RSV infection downregulates IL-21/IL-21R in Tfh cells via PD-L1 induction

PD-L1 is expressed on hematopoietic and nonhematopoietic cells; upon binding to PD-1 expressed in different cells, it delivers a signal with inhibitory effects for survival and function.<sup>22,23</sup> Tfh cells express PD-1 constitutively.<sup>24</sup> Previous studies demonstrated that RSV infection leads to PD-L1 upregulation in DCs.<sup>25</sup> PD-L1 upregulation in response to a helminth infection was reported to affect Tfh cells viability, leading to impairment of humoral responses.<sup>26</sup> In order to become fully differentiated Tfh cells, CD4<sup>+</sup> T cells need to receive first a signal from DCs in the T-cell zone and after that a signal from GC B cells in the GC.<sup>24</sup> We observed that not only DCs but also B cells in the lungs of RSV-infected mice upregulated PD-L1 (Figure 1a, b, Supplementary figure 2a).

IL-21 is one of the main signals delivered by Tfh cells to GC B cells to activate the production of high-affinity antibodies.<sup>16,27</sup> We next investigated whether RSV infection can modulate IL-21/IL-21R expression in Tfh cells. To test that, we infected mice with  $1 \times 10^7$  plaque-forming units (PFUs) of RSV and after 5 days analyzed the intracellular expression of IL-21 or the surface expression of IL-21R in Tfh cells. RSV-infected mice did not induce IL-21 in Tfh cells (Figure 1c, d) and downregulated the expression of IL-21R in both Tfh cells (Figure 1e, f) and in B cells (Supplementary figure 2b). However, treatment with anti-PD-L1 (Supplementary figure 1a) increased IL-21 (Figure 1c, d) and restored IL-21R expression (Figure 1e, f) in lung Tfh cells, and increased IL-21R expression in B cells (Supplementary figure 2b). Together, these results suggested that PD-L1 induction by RSV was indeed necessary to block IL-21 production.

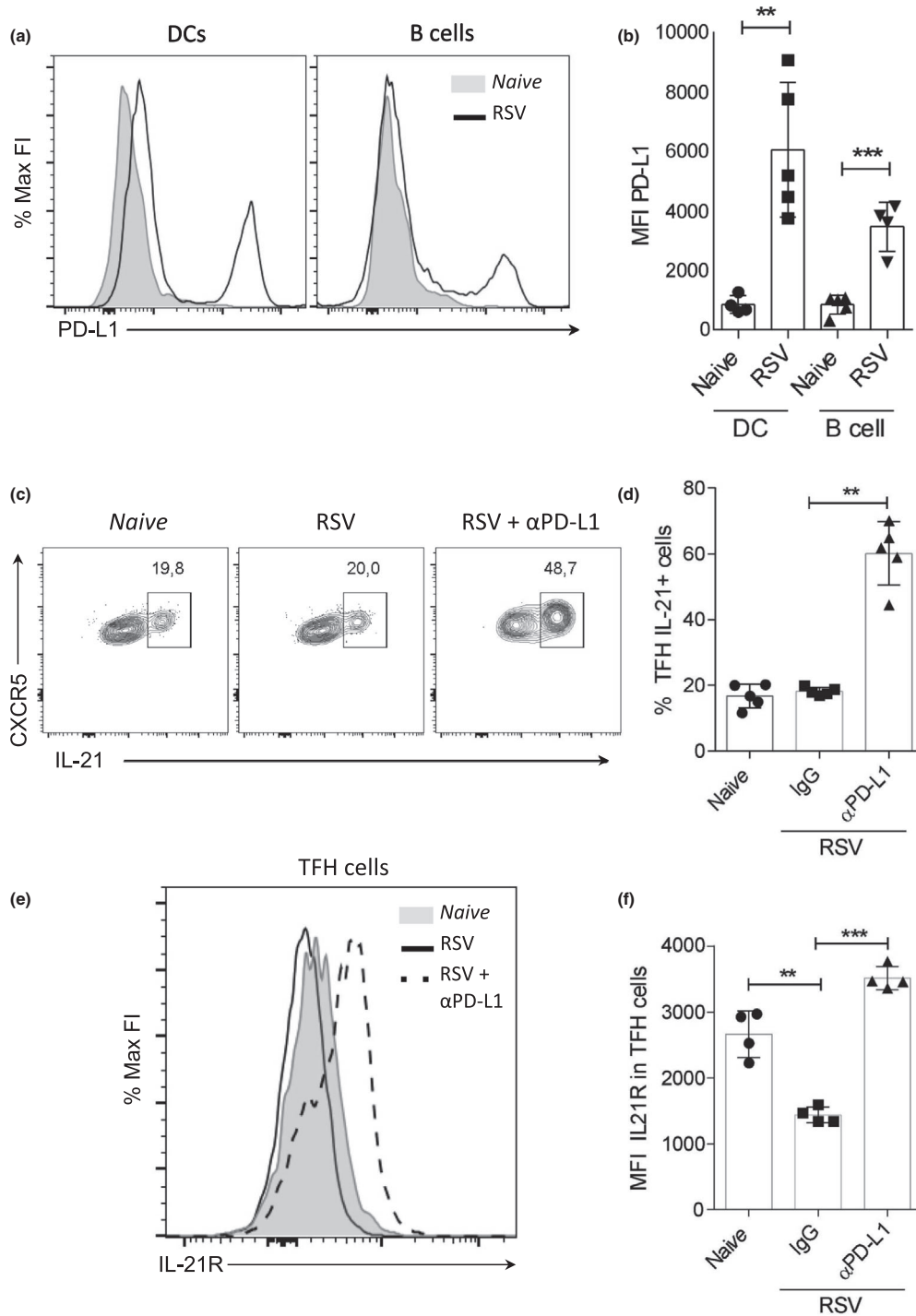


**Figure 1.** Programmed death-ligand 1 (PD-L1) blockade recovers interleukin (IL)-21/interleukin-21 receptor (IL-21R) expression in lung follicular helper T (Tfh) cells. BALB/c mice were intranasally infected with  $1 \times 10^7$  plaque-forming units (PFUs) of respiratory syncytial virus (RSV) and treated intraperitoneally with two doses of 200  $\mu$ g of anti-PD-L1 or isotype control on days 2 and 4 after infection. Five days after the infection, mice were killed and lungs were analyzed. **(a, b)** Mean fluorescence intensity (MFI) of PD-L1 in dendritic cells (DCs;  $CD45^+CD11c^+CD19^-$ ) and B ( $CD45^+CD11c^-CD19^+$ ) cells in RSV-infected or non-infected mice. **(c and d)** Gating and percentage of IL-21 expression or percentage of IL-21<sup>+</sup> in Tfh ( $CD45^+CD4^+CXCR5^+PD1^+$ ) cells in naive, RSV-infected or RSV-infected and treated with anti-PD-L1 mice. Results representative of three experiments, using five mice per experimental group. \*\* $P < 0.01$ ; \*\*\* $P < 0.001$ .

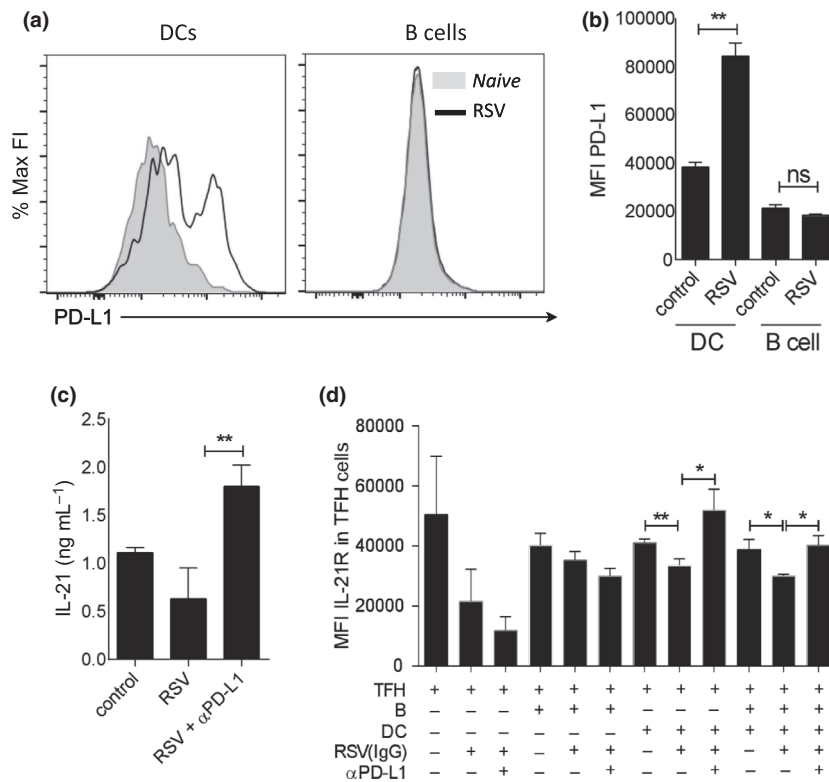


**Figure 2.** *In vitro* programmed death-ligand 1 (PD-L1) blockade recovers interleukin (IL)-21/interleukin-21 receptor (IL-21R) expression on follicular helper T (Tfh) cells in a dendritic cell (DC)-dependent manner. DCs (CD11c<sup>+</sup>CD19<sup>-</sup>), B cells (CD11c<sup>-</sup>CD19<sup>+</sup>) and Tfh cells (CD4<sup>+</sup>CXCR5<sup>+</sup>PD1<sup>+</sup>) from BALB/c mice splenocytes were sorted, cocultured in different combinations and incubated with respiratory syncytial virus (RSV) and/or αPD-L1 for 4 days. **(a and b)** Mean fluorescence intensity (MFI) of PD-L1 in sorted DCs and B cells, in the presence or absence of RSV. **(c)** Supernatant IL-21 quantification from coculture of B cells, DCs and Tfh incubated with RSV and αPD-L1. **(d)** IL-21R MFI in Tfh cells from cocultures in different combinations of sorted B cells and DCs. Undetectable levels were considered zero for statistical purposes. The experiment was performed in triplicates. \**P* < 0.05; \*\**P* < 0.01. ns, not significant.

We next investigated whether PD-L1 upregulation in B cells and DCs was caused by a direct interaction of RSV with either of these cell populations. To answer this question, we sorted DCs and B cells and incubated them *in vitro* with RSV. Only DCs upregulated PD-L1 expression as a direct effect of RSV, expressing higher PD-L1 levels compared with B cells (Figure 2a, b). We hypothesized that, if DCs were the main direct RSV target for PD-L1 induction, blocking this signal would restore IL-21 and IL-21R levels in Tfh only if DCs were in the culture. We again sorted Tfh, DCs and B cells, and incubated them with RSV in different combinations. IL-21 production could only be detected upon PD-L1 blockade (Figure 2c). Interestingly, IL-21R expression was only recovered in Tfh cells upon PD-L1 blockade when cultured in the presence of DCs (Figure 2d) but not by Tfh cells when cultured exclusively with B cells. These results suggested that the direct induction of PD-L1 by RSV in DCs, but not B cells, could constitute a key

mechanism of inhibition of the IL-21–IL-21R axis in Tfh cells, and this can be reversed by anti-PD-L1 treatment.

### IL-21 treatment increases Tfh and reduces Tfr cell numbers in lungs upon RSV infection

Our results indicated that RSV interfered in the signaling between the IL-21–IL-21R and PD-1–PD-L1 pathways, inhibiting the development of an efficient humoral response against the virus. Although we had observed that PD-L1 blockade recovered IL-21 and IL-21R levels, a previous study had shown that this approach was not useful *in vivo*.<sup>28</sup> In that study, anti-PD-L1 treatment in RSV-infected mice induced proinflammatory cytokines, exacerbating pulmonary inflammation and host disease, leading to a moderate enhancement of Tfh cells numbers, and no improvement of antibody responses was observed up to 6 days following infection. Under the hypothesis that IL-21 modulation was connected to PD-L1 expression, we

decided to test an alternative approach, treating RSV-infected mice with recombinant, endotoxin-free IL-21 (Supplementary figure 1b). In the lungs, RSV infection decreased the percentages of Tfh cells (Figure 3a), contrary to what was observed in LDLNs. Furthermore, the absolute number of Tfh cells in the lung of naïve animals was low, and RSV infection was not able to increase this. IL-21 treatment increased the absolute numbers of Tfh cells in the lungs and LDLNs (Supplementary figure 3b) and partially restored Tfh cell percentages during RSV infection in the lungs (Figure 3a), with no effect in LDLNs.

In addition, we observed that Tfr cell percentages and absolute numbers were expanded in RSV-infected mice in both LDLNs and lungs (Figure 3b and Supplementary figure 3c). Tfr cells negatively regulate Tfh cell functions and are defined phenotypically as CXCR5<sup>+</sup>PD1<sup>+</sup>CD4<sup>+</sup>Foxp3<sup>+</sup> T cells.<sup>29,30</sup> IL-21 treatment reversed this, decreasing Tfr cells numbers (Figure 3b and Supplementary figure 3c). Our data suggest that RSV can increase the relative percentages of Tfr/Tfh cells, and one of the mechanisms by which IL-21 treatment increases Tfh numbers in RSV infection *in vivo* might be the reduction of Tfr cells.

#### **IL-21 treatment induces TLOs formation and neutralizing antibody responses, reducing severity of RSV infection**

A logical prediction from these findings was that if IL-21 treatment could restore Tfh function *in vivo*, a direct effect would be observed over B cells and the anti-RSV antibody response. Accordingly, we observed that treatment with IL-21 in RSV-infected mice was able to induce the formation of TLOs resembling GCs inside of the lungs (Figure 4a). TLOs are ectopic lymphoid structures congregating mainly B and T cells, observed during acute inflammatory reactions, in infections, autoimmune disease and even cancer, and are associated with a protective response.<sup>31</sup> Moreover, IL-21 treatment increased proliferation capacity of total B cells in LDLNs and lungs (Supplementary figure 4a–c). It also resulted in increased titers of anti-F IgG (Figure 4b) and IgA (Figure 4c) in bronchoalveolar lavage starting at day 14 after infection. Finally, it increased anti-F IgG in serum (Figure 4d) and avidity of anti-RSV IgG (Figure 4e).

We then tested whether the antibodies produced upon IL-21 treatment would mediate reduction of severity in RSV infection. A hallmark of RSV infection is inflammatory pulmonary injury in peribronchial and perivascular areas (Figure 5a, b). Treatment with IL-21 reduced both peribronchial and perivascular inflammation (Figure 5a, b). IL-21 treatment also decreased numbers of RSV copies in lungs in RSV-

infected mice (Figure 5c) and weight loss (Supplementary figure 1c) of infected animals, compared with untreated infected mice.

We next tested the neutralization capacity of the antibodies in the serum of RSV-infected mice *versus* serum of IL-21-treated mice, in Vero cells. Sera from IL-21-treated mice showed a significantly enhanced neutralization power (Figure 5d). To evaluate the protective potential of the generated antibodies, we pretreated naïve mice with purified IgG from serum of naïve mice or RSV-infected mice, either treated or not with IL-21, 2 days prior to RSV infection, and measured viral copies in lungs at day 5 after infection. The results indicated that a partial protection to RSV infection could be mediated by IgG alone, elicited by IL-21 treatment in infected mice (Figure 5e).

## **DISCUSSION**

In this study, we unveil a pathway by which RSV can evade effector immune responses, impairing the generation of protective antibodies by inhibiting Tfh cell function, mainly the production of IL-21. Different studies report that targeting differentiation and/or function of immune cells constitutes a major virulence strategy for different viruses. Lymphocytic choriomeningitis virus negatively modulates antibody responses by killing Tfh cells via natural killer cell cytotoxicity.<sup>32</sup> Human immunodeficiency virus (HIV) infection is associated with a decrease in follicular regulatory T cell (Tfr cell) function, leading to Tfh cell proliferation, which is the major HIV-producing CD4<sup>+</sup> T-cell subpopulation, and consequently increasing viral replication.<sup>33</sup> Until now, modulation of Tfh cells by RSV had not been reported; and Tfh frequencies in humans during an RSV infection have not yet been described.

The production of IL-21 by Tfh cells coordinates the GC reaction and generation of high-affinity antibodies. The presence of RSV-specific high-affinity antibodies is associated with protection against RSV infection in infants under 3 months old.<sup>6</sup> Respiratory infections such as influenza are known to increase IL-21 production and Tfh cell responses.<sup>34</sup> However, the influence of IL-21 treatment during RSV infection was so far unexplored. Our studies demonstrated that IL-21 production by Tfh cells is inhibited specifically by RSV. In line with our findings, a cohort study that characterized the primary and secondary cytokine response to RSV infection did not detect IL-21 in swab nasal secretion samples from infants recruited during two consecutive winters.<sup>35</sup> Another study<sup>36</sup> demonstrated that IL-21 depletion during priming exacerbates immunopathology in mice

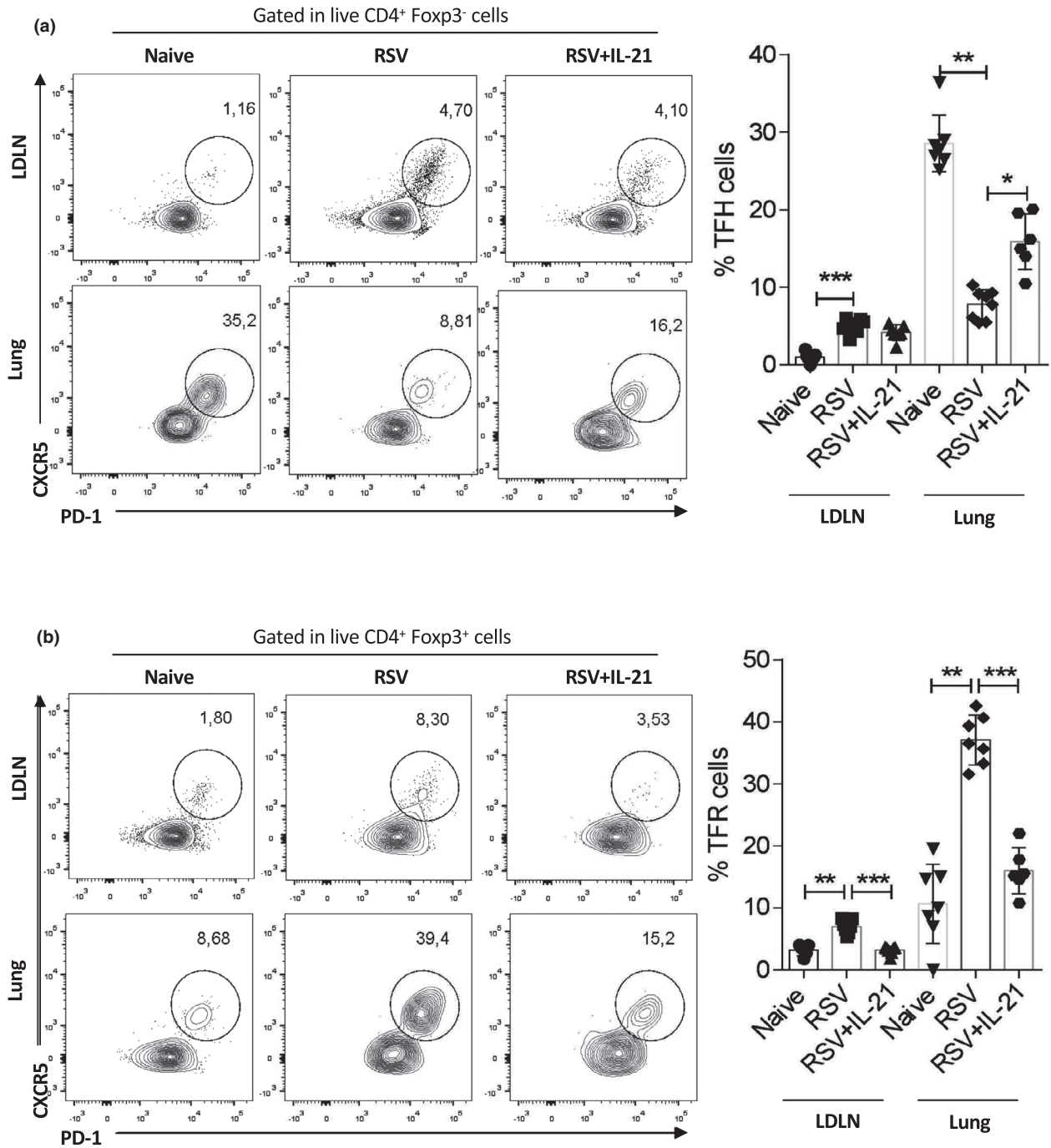


**Figure 3.** *In vivo* interleukin (IL)-21 treatment recovers the Tfr-to-Tfh ratio in lungs. BALB/c mice were intranasally infected with  $1 \times 10^7$  plaque-forming units (PFUs) of respiratory syncytial virus (RSV) and treated subcutaneously with four doses of 0.5  $\mu$ g of IL-21. (a) Representative gates of Tfh cells (CD45<sup>+</sup>CD4<sup>+</sup>FOXP3<sup>-</sup>CXCR5<sup>+</sup>PD-1<sup>+</sup>) and quantification of Tfh cell percentages in lung draining lymph nodes (LDLNs) and lungs. (b) Representative gate of Tfr cells (CD45<sup>+</sup>CD4<sup>+</sup>FOXP3<sup>+</sup>CXCR5<sup>+</sup>PD-1<sup>+</sup>) and Tfr cell percentages in LDLNs and lungs. Results show pooled data from two or three independent experiments, with  $n = 5-7$  mice per group. \* $P < 0.05$ ; \*\* $P < 0.01$ ; \*\*\* $P < 0.001$ . PD-1, programmed cell death protein 1; Tfh, follicular helper T; Tfr, regulatory follicular T (cell).



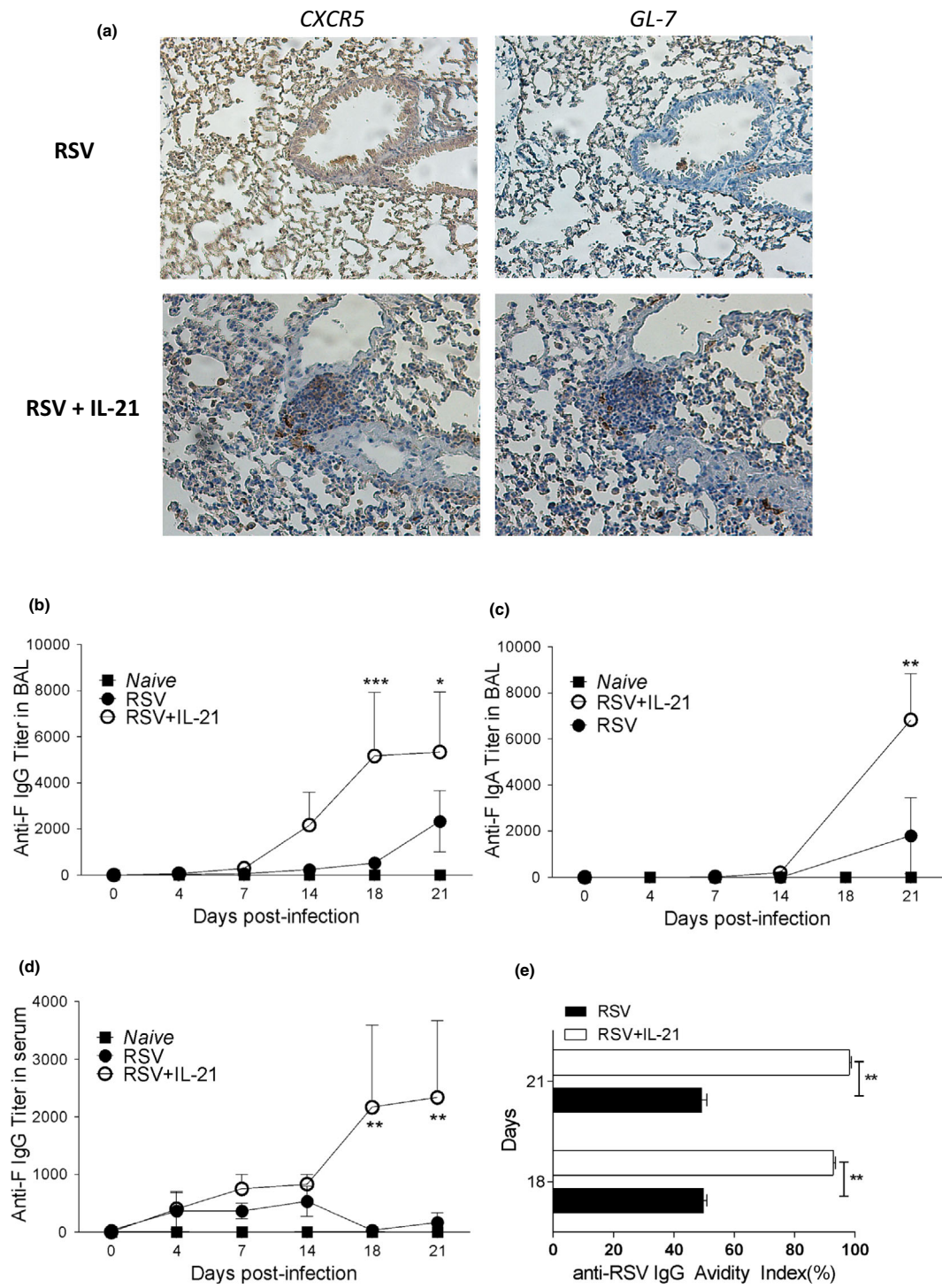


**Figure 4.** *In vivo* interleukin (IL)-21 treatment increases specific-antibody responses in respiratory syncytial virus (RSV)-infected mice. BALB/c mice were intranasally infected with  $1 \times 10^7$  plaque-forming units (PFUs) of RSV and treated subcutaneously with four doses of 0.5  $\mu$ g of IL-21. (a) Ectopic lymphoid formation in lung stained by CXCR5 and GL-7. (b) Anti-F IgG titers measured by ELISA in bronchoalveolar lavage (BAL). (c) Anti-F IgA titers measured by ELISA in BAL. (d) Anti-F IgG titers measured by ELISA in serum. (e) Total IgG avidity index on days 18 and 21 after infection. Results show pooled data from two or three independent experiments, with  $n = 3$  or 5 mice per group. \* $P < 0.05$ ; \*\* $P < 0.01$ ; \*\*\* $P < 0.001$ . Ig, immunoglobulin.

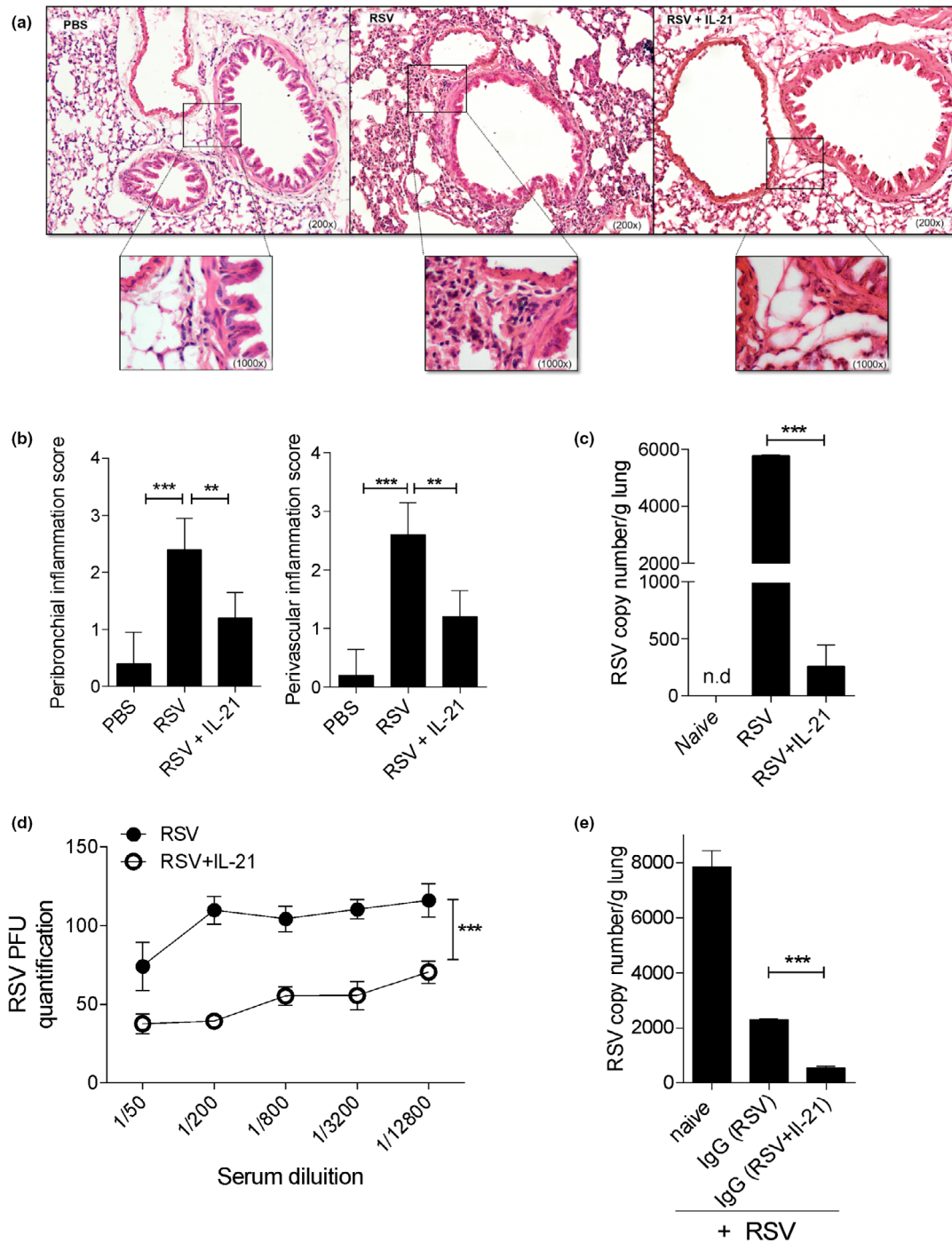


**Figure 5.** *In vivo* interleukin (IL-21) treatment decreases respiratory syncytial virus (RSV) titers and lung inflammation. BALB/c mice were intranasally infected with  $1 \times 10^7$  plaque-forming units (PFUs) of RSV and treated subcutaneously with four doses of  $0.5 \mu\text{g}$  of IL-21. **(a)** Lung hematoxylin and eosin histology (200x and 1000x magnification), 21 days after infection. **(b)** Peribronchial and perivascular inflammation score. **(c)** Real-time (RT)-PCR quantification of RSV copies in the lungs, 21 days after infection. **(d)** *In vitro* neutralization capacity assay. **(e)** Passive immunization with purified IgG from RSV-infected mice or IL-21-treated RSV-infected mice for which RSV copies were measured in the lungs by RT-PCR. Results show pooled data from two or three independent experiments, with  $n = 3$  or 5 mice per group.  $**P < 0.01$ ;  $***P < 0.001$ . n.d., not detected; PBS, phosphate-buffered saline.



after RSV challenge, and reduces antibody production, evidencing a major role for IL-21 in RSV infection.

In fact, inhibition of IL-21 expression is a strategy employed by different pathogens to evade effector immune responses. In hepatitis C virus patients, serum IL-21 levels and the frequency of IL-21-producing Tfh cells in blood were found to be lower compared with healthy individuals.<sup>37</sup> Lower frequencies of IL-21-producing CD4<sup>+</sup> T cells were also associated with reduced proliferation and increased expression of the inhibitory receptors such as CTLA-4, Tim-3 and PD-1 on hepatitis C virus-specific CD8<sup>+</sup> T cells in a viral-persistence state.<sup>38</sup> In fact, IL-21 has potent and specific effects on mucosal antiviral responses, assisting viral clearance and regulating pulmonary T- and B-cell responses.<sup>39</sup> IL-21 treatment has been tested against several types of viral pathogens, such as hepatitis B virus,<sup>40</sup> hepatitis C virus<sup>38</sup> and HIV.<sup>41,42</sup> IL-21 knockout mice are profoundly impaired in B-cell responses, with reduced plasma cell formation and GC function, decreased B-cell proliferation, transition into memory B cells and antibody affinity maturation.<sup>43</sup> In addition, IL-21 induces IL-21R expression on activated B cells and Tfh cells.<sup>44-46</sup> All these studies underline the relevance of IL-21 for the generation of protective antibodies. In our study, RSV infection led to impairment of IL-21 expression in lung Tfh cells, whereas IL-21 treatment resulted in more efficient GC response, decreasing Tfr cells, increasing Tfh and B cells numbers as well as leading to the production of IgA and IgG antibodies that protected naïve animals that were challenged *in vivo* by RSV. Although our data do not show that the improved antibody response against RSV is dependent on the IL-21-recovered Tfh cell function, they demonstrate the strong correlation between the two phenomena.

When we investigated the lungs of RSV-infected mice at day 21 after infection, we did not observe the presence of TLOs. The RSV-infected mice that were treated with IL-21, however, showed TLOs mostly around the bronchi regions, with positive staining for CXCR5 and GL-7. Such tertiary structures are commonly observed in respiratory infections such as influenza.<sup>47,48</sup> In particular, mice lacking peripheral lymphoid organs and infected with high titers of influenza virus are able to organize B and T cells ectopically, in tissues, and thus clear the infection, highlighting the importance of TLOs as a local protective immune response.<sup>49</sup> The formation of TLOs is also observed in target organs of autoimmune disease, transplanted organs, solid tumors and chronic inflammation tissues (see the review by Luo *et al.*<sup>50</sup>). In human renal allograft rejection, TLO formation in grafts is dependent on IL-21.<sup>51</sup> One of the functional roles of TLOs is sustaining the generation of antibody responses.

Our data support a role for IL-21 in inducing TLO formation and a protective antibody response against RSV infection.

We also observed that IL-21R was downregulated on lung Tfh cells in RSV-infected mice. This observation is consistent with the inhibition of IL-21 production by RSV. In humans, IL-21R defects cause severe primary immunodeficiency and reduced activity of natural killer, T and B cells, resulting in multiple infections.<sup>52</sup> Our results indicate that the downregulation of IL-21R is another important mechanism associated with the impairment of B-cell responses against RSV in mice, evidencing the relevance of the IL-21–IL-21R axis in the generation of protection to this virus.

Finally, we found that inhibition of IL-21 production during RSV infection depended on PD-L1 induction. Tfh cells naturally express PD-1.<sup>12</sup> PD-L1, one of the classic PD-1 ligands, is responsible for immune homeostasis, negatively modulating PD-1-expressing T cells<sup>53</sup> and B cells.<sup>54</sup> PD-1–PD-L1 interactions reduce Akt phosphorylation in PD-1-expressing cells, leading to decreases in function and cell survival.<sup>55</sup> PD-L1 expression in RSV-infected patients has not been described; however, PD-L1 has been previously reported to be increased in DCs<sup>25,56</sup> and B cells<sup>28</sup> of mice and also in bronchial epithelial human cells line<sup>57</sup> infected with RSV. PD-1 is usually studied with regard to its expression in T cells and used here as a marker for Tfh cells; however, different studies have reported that PD-1 can also be upregulated in DCs<sup>58-60</sup> and B cells,<sup>61,62</sup> where it can relay inhibitory signals for these cells as well. Our findings showed that RSV induced the expression of PD-L1 in lung DCs and B cells, and treatment with anti-PD-L1 restored the expression of IL-21/IL-21R in lung Tfh cells. In addition, our *in vitro* experiments showed that RSV could directly upregulate PD-L1 expression in DCs, but in not B cells. Similar to our findings regarding the role of PD-L1 and IL-21 in RSV infection, Cubas *et al.* demonstrated that HIV infection increased PD-L1 frequency in GC B cells leading to reduction of Tfh cell proliferation and IL-21 production.<sup>63</sup> Upregulation of PD-L1 in B cells mediated by RSV depended on DCs and T cells. It is possible that the mechanism by which PD-1–PD-L1 interactions inhibit Tfh cells function is by downregulation of c-Maf expression in these cells, a transcriptional factor involved in transactivation of both the promoter and enhancer of the IL-21 gene, and is inversely associated with PD-L1 expression.<sup>24,64</sup> We did not explore the capacity of RSV to induce PD-L1 expression in Tfh cells, which have been already shown to play a role in a colitis mice model.<sup>65</sup> PD-L1 upregulation in Tfh cells could be another important pathway to affect Tfh-cell function, decreasing IL-21 production. Several

studies have also suggested that blockade of PD-1 or PD-L1 may lead to a reversion of T-cell dysfunction in the context of chronic infection.<sup>66</sup> PD-L1 blockade in regulatory B cells can recover Th1 cell activity in visceral leishmaniasis in a canine model.<sup>67</sup> When we blocked PD-L1 *in vitro* during RSV infection, IL-21 secretion was also increased, supporting our *in vivo* data. We suggest that an early course of IL-21 therapy, rather than anti-PD-L1 or anti-PD-1, might constitute a better approach to circumvent Tfh-cell functional impairment resulting from RSV infection. Treatment with anti-PD-L1 has been previously reported to lead to high inflammatory responses in RSV infection<sup>28</sup>; more recently, in cancer patients with COVID-19 (coronavirus disease 2019), treatment with anti-PD-1 also resulted in exacerbated lung inflammation.<sup>68</sup> Before we can think of the use of anti-PD-1/PD-L1 antibodies as a viable approach for therapy in viral infections, more information is needed on the multiple signals these will affect in T, DC and B cells that may coexpress both markers in these situations.

In summary, our data underline the importance of IL-21 and highlight an intricate connection between the IL-21–IL-21R and the PD-1–PD-L1 axis in the regulation of Tfh- and Tfr-cell function for the development of a protective humoral response during RSV infection. Further investigation of this pathway, as well as clinical studies of IL-21 treatment in RSV-infected patients, will contribute to the development of new vaccine strategies, as well as immunotherapy, against respiratory infections.

## METHODS

### Viruses and cells

Vero cells (ATCC CCL81) were cultured in Dulbecco's modified Eagle's medium (Gibco, USA) supplemented with 10% fetal calf serum (Gibco, USA) and gentamicin (0.08 mg mL<sup>-1</sup>; Novafarma, Brazil), maintained at 37°C with 5% of CO<sub>2</sub>. These cells were used to propagate the RSV A2 strain. Viral PFUs were quantified using an RSV F protein-specific antibody (Millipore, Billerica, MA, USA). The virus produced was inactivated by UV light exposure for 30 min, at room temperature.

### Animals

Female BALB/c mice aged 6–8 weeks were purchased from the Biological Center of Experimental Models (CEMBE) at Pontifícia Universidade Católica do Rio Grande do Sul. A well-established model to study RSV infection was previously developed in the BALB/c strain.<sup>69</sup> Mice were housed at the Biological Center of Experimental Models (CEMBE) facility and received water and food *ad libitum*. All animal procedures were performed in accordance with the guidelines of the Federation of Brazilian Societies for Experimental Biology and

approved by the Pontifícia Universidade Católica do Rio Grande do Sul Ethics Committee for the Use of Animals (protocol number #13/00341).

### Infection and treatment

For *in vitro* infection, a single-cell suspension of splenocytes was obtained, stained with specific antibodies for DCs (CD11c<sup>+</sup>CD19<sup>-</sup>), B cells (CD19<sup>+</sup>CD11c<sup>-</sup>) and Tfh cells (CD4<sup>+</sup>CXCR5<sup>+</sup>PD-1<sup>+</sup>) and sorted. Sorted cells were cocultured (5 × 10<sup>3</sup> DCs, 3 × 10<sup>4</sup> Tfh cells or 5 × 10<sup>4</sup> B cells per well) in different combinations, and later infected with 1 × 10<sup>2</sup> PFUs mL<sup>-1</sup> of RSV for 4 days. In some experiments, 0.5 µg of anti-PD-L1 antibody (clone MHI5; eBioscience, USA) or IgG isotype control (Bio X Cell, USA) was added to the cultures, followed by analysis of IL-21R and PD-L1 expression.

For *in vivo* infection, mice were divided in four groups: two groups were infected intranasally with 1 × 10<sup>7</sup> PFUs of RSV, with one of them receiving subcutaneous over-the-shoulders treatment with 0.5 µg of recombinant IL-21 (eBioscience, USA) diluted in 100 µL of phosphate-buffered saline (PBS). The other two groups received PBS intranasally, with one of them subcutaneously administered recombinant IL-21. IL-21 was administered on days 2, 4, 8, 14 and 18 after infection. In some experiments, mice were treated on days 2 and 4 with 200 µg anti-PD-L1 antibody (clone MHI5, eBioscience, USA) or IgG isotype control (Bio X Cell, USA), both diluted in PBS. Bronchoalveolar lavage and blood collection occurred on days 0, 7, 14 and 21 after infection. Mice were killed at day 5 or 21 after infection; spleens, lungs and LDLNs were harvested for further analysis.

### ELISA

The concentrations of murine IL-21 were determined by capture ELISA (R&D Systems, USA), according to the manufacturer's instructions. Undetectable levels were considered zero for statistical purposes. For quantification of IgG and IgA RSV-specific antibodies in mice serum and bronchoalveolar lavage, 96-well plates were sensitized overnight with RSV F protein (Sino Biological Inc, USA), washed and blocked for 1 h with blocking buffer (5% milk + 0.05% tween in PBS 1× buffer) and serum or bronchoalveolar lavage was added in dilutions of 1/10, 1/100, 1/500, 1/1000, 1/10 000 and incubated for 2 h at room temperature. Rabbit antimouse IgG or IgA antibody, both horseradish peroxidase conjugated (Invitrogen, USA), followed by 3, 3', 5, 5' - Tetramethylbenzidine (TMB) (Life Technologies, Brazil) were used to develop the assay. Plates were read at 450 nm using an EZ Read 400 Microplate reader (Biochrom).

An ELISA to measure the avidity of anti-RSV antibody was conducted as described above; however, plates were washed with 6 M urea–PBS. The results were expressed as an Avidity Index, which was calculated as previously described.<sup>6</sup> The avidity of RSV-specific total IgG was classified according to values that had been predetermined arbitrarily, defined as low (<50%), intermediate (50–70%) or high (>70%).

### Neutralization assay

An assay to determine antibody neutralization capacity was performed as previously described.<sup>70</sup> Briefly, fourfold serial serum dilutions from 1:10 to 1:10 240 were prepared in virus diluent (Dulbecco's Modified Eagle Medium supplemented with 0% fetal calf serum and 1% gentamicin, 0.08 mg mL<sup>-1</sup>; Novafarma). Serially diluted serum was challenged with an equal volume of the RSV-A2 strain, previously titrated to give approximately 150 PFUs per 50  $\mu$ L of inoculum. The serum-virus mixtures were incubated at 37°C, 5% CO<sub>2</sub> for 1 h. Vero cells were seeded in 96-well plates, grown to a monolayer and then infected with 50  $\mu$ L per well (in triplicates) of the serum-virus mixture. Plates were kept with 0.5% methyl cellulose, prepared in Dulbecco's Modified Eagle Medium with 2% fetal bovine serum and incubated at 37°C, 5% CO<sub>2</sub> for 3 days to allow plaque formation. To observe the syncytium formation, wells were incubated with primary anti-RSV antibodies (Millipore, USA) and secondary antibody (horseradish peroxidase rabbit antimouse IgG; Millipore, USA) for 1 h at 37°C. Nonspecific binding was blocked with a blocking buffer. The assay was developed with 4-chloro-1-naphthol with 0.01% H<sub>2</sub>O<sub>2</sub> for 20 min in the dark. Syncytia were counted in an optical microscope and PFUs were calculated by the number of syncytia divided by the product of the virus dilution and the total volume in the well.

### Flow cytometry

Cells were labeled with anti-CD3 (APC-C7, 17A2 clone), anti-CD27 (APC, LG.3A10 clone), anti-FOXP3 (PE, MF23 clone), anti-B220 (PerCP, RA3-6B2 clone), anti-CD8a (APC-H7 536.7 clone), anti-IL-21R (PE, 4A9 clone) and anti-CD19 (APC-Cy7, ID3 clone) from BD Biosciences; anti-CD4 (eFluor710-PerCP, clone RM4-5), anti-PD-1 (PE-Cyanine7, clone J43), anti-Bcl-6 (PE, mgl191E clone), anti-CXCR5 (APC, clone SPRCL5), anti-ICOS (FITC, clone 7E17G9), anti-CD45 (FITC, clone 30-F11) and anti-CD274 (PE, clone MIH5) from eBioscience; anti-CD25 (PE, PC61 clone), anti-GL7 (FITC, GL7 clone), anti-CD11c (PE/Cy7 N418 clone) and anti-Ki67 (PE or PerCP, clone 16A8) from BioLegend. Viability was determined with Fixable Viability Dye eFluor 780 or 450 from eBioscience. For intracellular staining, we used Foxp3 staining buffer set (eBioscience). Cells were analyzed using an FACSCanto II (BD Biosciences) with the FACSDiva software (BD Biosciences). Sorting was performed in an FASCARIA (BD Biosciences).

### Histology and immunohistochemistry

Lungs and spleens were fixed with 10% formalin, embedded in paraffin and cut into 5- $\mu$ m sections (Olympus CUT 4060E). Hematoxylin and eosin staining was performed on sections to evaluate the cell infiltration and determine the inflammation scores. The score for peribronchial and perivascular inflammation was evaluated on a subjective scale of 0–3, as previously described.<sup>71</sup> Zero was attributed when no inflammation was detectable, 1 was attributed when occasional cuffing with inflammatory cells was observed, a value of 2 was given when most bronchi or vessels were surrounded by a thin

layer (one to five cells thick) of inflammatory cells and a value of 3 was given when most bronchi or vessels were surrounded by a thick layer (more than five cells thick) of inflammatory cells.

For immunohistochemistry, sections were deparaffinized with xylol and endogenous peroxidase activity was blocked by incubation with 3% H<sub>2</sub>O<sub>2</sub> in methanol. Antigen unmasking was performed by incubating the slides in 0.1 mol L<sup>-1</sup> citrate buffer, pH 6, for 30 min at 95°C, followed by cooling at room temperature for 1 h. Sections were blocked in PBS with 4% bovine serum albumin and 5% mouse serum and later incubated with primary antibody anti-CXCR5 (clone 2G8, BD Biosciences) or anti-GL-7 (GL7 clone, Invitrogen) at a 1:500 dilution in PBS with 1% bovine serum albumin and 1.25% mouse serum. Biotinylated goat-derived secondary antibodies were detected by the avidin-biotin-horseradish peroxidase complex method (Dako Systems) using 3,3'-diaminobenzidine-tetrahydrochloride (Sigma-Aldrich) as a substrate.

### Real-Time PCR

Total RNA was extracted from the lungs of infected animals using the Viral RNA/DNA Mini Kit (PureLink; Invitrogen, Canada) following the manufacturer's instructions. Complementary DNA was synthesized using random primers and the Sensiscript Reverse Transcription kit (QIAGEN, USA). The quality of complementary DNA for each sample was evaluated by amplification of the endogenous  $\beta$ -actin gene. Samples that did not amplify for  $\beta$ -actin were excluded. Real-time PCR was performed for the amplification of the RSV F protein gene using the primers and specific probes (forward-5'-AACAGATGTAAGCAGCTCCGTTATC-3', reverse-5'-GATTTTTATTGGATGCTGTACATTT-3' and probe 5'-FAM/TGCCATAGCATGACACAATGGCTCCT-TAMRA-3'). For the standard curve, ten-fold serial dilutions of  $6 \times 10^7$  copies of a plasmid with the RSV F protein gene sequence were added to the same plate of quantitative PCR in duplicate. The results were measured by the StepOne Real-Time PCR System (Applied Biosystems) and used for further quantification of the samples viral load.

### Passive immunization

Serum IgG from mice was purified using a Protein A-Sepharose column (Sigma, USA) following manufacturer's instructions. Mice were separated into three groups: the first group received IgG serum from RSV-infected mice, the second group received IgG serum from RSV-infected/IL-21-treated mice and the third group received serum from naïve mice. Each mouse received 300  $\mu$ g of purified IgG intraperitoneally. After 2 days, animals were infected with  $1 \times 10^7$  PFUs of RSV intranasally. Mice were killed at day 5 after infection and lungs were harvested for further analysis.

### Statistical analysis

Data were tested for normal distribution using a Kolmogorov-Smirnov test; differences between the groups were analyzed with one-way analysis of variance (ANOVA) followed by a

Bonferroni post-test, or paired *t*-tests using GraphPad Prism software (San Diego, CA, USA). Values demonstrated in graphs are the mean  $\pm$  the standard deviation (s.d.). A level of significance of  $P < 0.05$  was established for the analyses.

## ACKNOWLEDGMENTS

This study was supported by grants from Conselho Nacional de Desenvolvimento Científico e Tecnológico (CNPq), Fundação de Pesquisa do Estado do Rio Grande do Sul (FAPERGS), Coordenação de Aperfeiçoamento de Pessoal de Nível Superior – Brasil (CAPES) and Pontifícia Universidade Católica do Rio Grande do Sul.

## CONFLICT OF INTEREST

The authors declared no potential conflicts of interest with respect to the research, authorship and/or publication of this article.

## REFERENCES

- Shi T, McAllister DA, O'Brien KL, *et al.* Global, regional, and national disease burden estimates of acute lower respiratory infections due to respiratory syncytial virus in young children in 2015: a systematic review and modelling study. *Lancet* 2017; **390**: 946–958.
- Anderson LJ, Dormitzer PR, Nokes DJ, Rappuoli R, Roca A, Graham BS. Strategic priorities for respiratory syncytial virus (RSV) vaccine development. *Vaccine* 2013; **31**: B209–B215.
- Hall CB, Walsh EE, Long CE, Schnabel KC. Immunity to and frequency of reinfection with respiratory syncytial virus. *J Infect Dis* 1991; **163**: 693–698.
- DeVincenzo JP, Wilkinson T, Vaishnav A, *et al.* Viral load drives disease in humans experimentally infected with respiratory syncytial virus. *Am J Respir Crit Care Med* 2010; **182**: 1305–1314.
- Habibi MS, Jozwik A, Makris S, *et al.* Impaired antibody-mediated protection and defective IgA B-cell memory in experimental infection of adults with respiratory syncytial virus. *Am J Respir Crit Care Med* 2015; **191**: 1040–1049.
- Freitas GRO, Silva DAO, Yokosawa J, Paula NT, Costa LF, Carneiro BM. Antibody response and avidity of respiratory syncytial virus-specific total IgG, IgG1, and IgG3 in young children. *J Med Virol* 2011; **83**: 1826–1833.
- Sande CJ, Mutunga MN, Okiro EA, Medley GF, Cane PA, Nokes DJ. Kinetics of the neutralizing antibody response to respiratory syncytial virus infections in a birth cohort. *J Med Virol* 2013; **85**: 2020–2025.
- Falsey AR, Singh HK, Walsh EE. Serum antibody decay in adults following natural respiratory syncytial virus infection. *J Med Virol* 2006; **78**: 1493–1497.
- Jr JC. Respiratory syncytial virus vaccine development. *Vaccine* 2001; **10**: 1415–1433.
- McLellan JS, Chen M, Joyce MG, *et al.* Structure-based design of a fusion glycoprotein vaccine for respiratory syncytial virus. *Science* 2013; **342**: 592–598.
- Tian D, Battles MB, Moin SM, *et al.* Structural basis of respiratory syncytial virus subtype-dependent neutralization by an antibody targeting the fusion glycoprotein. *Nat Commun* 2017; **8**: 1877.
- Crotty S. Follicular helper CD4 T cells (TFH). *Annu Rev Immunol* 2011; **29**: 621–663.
- Weber JP, Fuhrmann F, Feist RK, *et al.* ICOS maintains the T follicular helper cell phenotype by down-regulating Krüppel-like factor 2. *J Exp Med* 2015; **212**: 217–233.
- Bentebibel S-E, Schmitt N, Banchereau J, Ueno H. Human tonsil B-cell lymphoma 6 (BCL6)-expressing CD4<sup>+</sup> T-cell subset specialized for B-cell help outside germinal centers. *Proc Natl Acad Sci USA* 2011; **108**: E488–E497.
- Bauquet AT, Jin H, Paterson AM, *et al.* Costimulatory molecule ICOS plays a critical role in the development of TH -17 and follicular T-helper cells by regulating c- Maf expression and IL-21 production. *Nat Immunol* 2009; **10**: 167–175.
- Linterman MA, Beaton L, Yu D, *et al.* IL-21 acts directly on B cells to regulate Bcl-6 expression and germinal center responses. *J Exp Med* 2010; **207**: 353–363.
- Zotos D, Coquet JM, Zhang Y, *et al.* IL-21 regulates germinal center B cell differentiation and proliferation through a B cell–intrinsic mechanism. *J Exp Med* 2010; **207**: 365–378.
- Nutt SL, Tarlinton DM. Germinal center B and follicular helper T cells: Siblings, cousins or just good friends? *Nat Immunol* 2011; **12**: 472–477.
- Chan TD, Brink R. Affinity-based selection and the germinal center response. *Immunol Rev* 2012; **247**: 11–23.
- Hou S, Clement RL, Diallo A, *et al.* FoxP3 and Ezh2 regulate Tfr cell suppressive function and transcriptional program. *J Exp Med* 2019; **216**: 605–620.
- Sage PT, Sharpe AH. T follicular regulatory cells in the regulation of B cell responses. *Trends Immunol* 2015; **36**: 410–418.
- Keir ME, Butte MJ, Freeman GJ, Sharpe AH. PD-1 and its ligands in tolerance and immunity. *Annu Rev Immunol* 2008; **26**: 677–704.
- Carter LL, Fouser LA, Jussif J, *et al.* PD-1:PD-L inhibitory pathway affects both CD4<sup>+</sup> and CD8<sup>+</sup> T cells and is overcome by IL-2. *Eur J Immunol* 2002; **32**: 634–643.
- Jogdand GM, Mohanty S, Devadas S. Regulators of Tfh cell differentiation. *Front Immunol* 2016; **7**: 1–14.
- Wang H, Peters N, Schwarze J. Plasmacytoid dendritic cells limit viral replication, pulmonary inflammation, and airway hyperresponsiveness in respiratory syncytial virus infection. *J Immunol* 2006; **177**: 6263–6270.
- Hams E, McCarron MJ, Amu S, *et al.* Blockade of B7–H1 (programmed death ligand 1) enhances humoral immunity by positively regulating the generation of T follicular helper cells. *J Immunol* 2011; **186**: 5648–55.
- Bansal RR, Mackay CR, Moser B, Eberl M. IL-21 enhances the potential of human  $\gamma\delta$  T cells to provide B-cell help. *Eur J Immunol* 2012; **42**: 110–119.
- Yao S, Jiang L, Moser EK, *et al.* Control of pathogenic effector T-cell activities in situ by PD-L1 expression on respiratory inflammatory dendritic cells during respiratory syncytial virus infection. *Mucosal Immunol* 2015; **8**: 746–759.

29. Wollenberg I, Agua-Doce A, Hernández A, *et al.* Regulation of the germinal center reaction by Foxp3<sup>+</sup> follicular regulatory T cells. *J Immunol* 2011; **187**: 4553–4560.
30. Alexander CM, Tygrett LT, Boyden AW, Wolniak KL, Legge KL, Waldschmidt TJ. T regulatory cells participate in the control of germinal center reactions. *Immunology* 2011; **133**: 452–468.
31. Sautès-Fridman C, Petitprez F, Calderaro J, Fridman WH. Tertiary lymphoid structures in the era of cancer immunotherapy. *Nat Rev Cancer* 2019; **19**: 307–325.
32. Cook KD, Kline HC, Whitmire JK. NK cells inhibit humoral immunity by reducing the abundance of CD4<sup>+</sup> T follicular helper cells during a chronic virus infection. *J Leukoc Biol* 2015; **98**: 153–162.
33. Chowdhury A, Del Rio PME, Tharp GK, *et al.* Decreased T Follicular Regulatory Cell/T Follicular Helper Cell (TFH) in Simian immunodeficiency virus-infected rhesus macaques may contribute to accumulation of TFH in chronic infection. *J Immunol* 2015; **195**: 3237–3247.
34. Karnowski A, Chevrier S, Belz GT, *et al.* B and T cells collaborate in antiviral responses via IL-6, IL-21, and transcriptional activator and coactivator, Oct2 and OBF-1. *J Exp Med* 2012; **209**: 2049–2064.
35. Ugonna K, Douros K, Bingle CD, Everard ML. Cytokine responses in primary and secondary respiratory syncytial virus infections. *Pediatr Res* 2016; **79**: 946–950.
36. Dodd JS, Clark D, Muir R, Korpis C, Openshaw PJM. Endogenous IL-21 regulates pathogenic mucosal CD4 T-cell responses during enhanced RSV disease in mice. *Mucosal Immunol* 2013; **6**: 704–717.
37. Spaan M, Kreeft K, de Graav GN, *et al.* CD4<sup>+</sup> CXCR5<sup>+</sup> T cells in chronic HCV infection produce less IL-21, yet are efficient at supporting B cell responses. *J Hepatol* 2015; **62**: 303–310.
38. Kared H, Fabre T, Bernard N, Bruneau J, Shoukry NH. Galectin-9 and IL-21 Mediate Cross-regulation between Th17 and Treg cells during Acute Hepatitis C. *PLoS Pathog* 2013; **9**: e1003422.
39. Spolski R, Leonard WJ. Interleukin-21: a double-edged sword with therapeutic potential. *Nat Rev Drug Discov* 2014; **13**: 379–395.
40. Li L, Liu M, Cheng L-W, *et al.* HBcAg-specific IL-21-producing CD4<sup>+</sup> T cells are associated with relative viral control in patients with chronic hepatitis B. *Scand J Immunol* 2013; **78**: 439–446.
41. Yue FY, Lo C, Sakhdari A, *et al.* HIV-specific IL-21 producing CD4<sup>+</sup> T cells are induced in acute and chronic progressive HIV infection and are associated with relative viral control. *J Immunol* 2010; **185**: 498–506.
42. Pallikkuth S, Pahwa S. Interleukin-21 and T follicular helper cells in HIV infection: research focus and future perspectives. *Immunol Res* 2013; **57**: 279–291.
43. Rankin AL, MacLeod H, Keegan S, *et al.* IL-21 receptor is critical for the development of memory B cell responses. *J Immunol* 2011; **186**: 667–674.
44. Avery DT, Deenick EK, Ma CS, *et al.* B cell-intrinsic signaling through IL-21 receptor and STAT3 is required for establishing long-lived antibody responses in humans. *J Exp Med* 2010; **207**: 155–171.
45. Nojima T, Haniuda K, Moutai T, *et al.* In-vitro derived germinal centre B cells differentially generate memory B or plasma cells *in vivo*. *Nat Commun* 2011; **2**: 465.
46. Caprioli F, Sarra M, Caruso R, *et al.* Autocrine regulation of IL-21 production in human T lymphocytes. *J Immunol* 2008; **180**: 1800–1807.
47. Geurtsvankessel CH, Willart MAM, Bergen IM, *et al.* Dendritic cells are crucial for maintenance of tertiary lymphoid structures in the lung of influenza virus-infected mice. *J Exp Med* 2009; **206**: 2339–2349.
48. Neyt K, GeurtsvanKessel CH, Deswarte K, Hammad H, Lambrecht BN. Early IL-1 signaling promotes iBALT induction after influenza virus infection. *Front Immunol* 2016; **7**: 312.
49. Moyron-Quiroz JE, Rangel-Moreno J, Kusser K, *et al.* Role of inducible bronchus associated lymphoid tissue (iBALT) in respiratory immunity. *Nat Med* 2004; **10**: 927–934.
50. Luo S, Zhu R, Yu T, *et al.* Chronic inflammation: a common promoter in tertiary lymphoid organ neogenesis. *Front Immunol* 2019; **10**: e 2938.
51. Deteix C, Attuil-Audenis V, Duthey A, *et al.* Intra-graft Th17 infiltrate promotes lymphoid neogenesis and hastens clinical chronic rejection. *J Immunol* 2010; **184**: 5344–5351.
52. Kotlarz D, Ziętara N, Milner JD, Klein C. Human IL-21 and IL-21R deficiencies. *Curr Opin Pediatr* 2014; **26**: 704–712.
53. Wherry EJ. T cell exhaustion. *Nat Immunol* 2011; **131**: 492–499.
54. Okazaki T, Maeda A, Nishimura H, Kurosaki T, Honjo T. PD-1 immunoreceptor inhibits B cell receptor-mediated signaling by recruiting src homology 2-domain-containing tyrosine phosphatase 2 to phosphotyrosine. *Proc Natl Acad Sci USA* 2001; **98**: 13866–13871.
55. Okazaki T, Honjo T. The PD-1-PD-L pathway in immunological tolerance. *Trends Immunol* 2006; **27**: 195–201.
56. Sow FB, Gallup JM, Krishnan S, Patera AC, Suzich J, Ackermann MR. Respiratory syncytial virus infection is associated with an altered innate immunity and a heightened pro-inflammatory response in the lungs of preterm lambs. *Respir Res* 2011; **12**: 106.
57. Telcian AG, Laza-Stanca V, Edwards MR, *et al.* RSV-induced bronchial epithelial cell PD-L1 expression inhibits CD8<sup>+</sup> T cell nonspecific antiviral activity. *J Infect Dis* 2011; **203**: 85–94.
58. Versteven M, Van den Bergh JMJ, Marcq E, *et al.* Dendritic cells and programmed death-1 blockade: a joint venture to combat cancer. *Front Immunol* 2018; **9**: e 394.
59. Garcia-Bates TM, Palma ML, Shen C, *et al.* Contrasting roles of the PD-1 signaling pathway in dendritic effector T. *Cell Functions*. 2019; **93**: e02035–18.
60. Lim TS, Chew V, Sieow JL, *et al.* PD-1 expression on dendritic cells suppresses CD8<sup>+</sup> T cell function and antitumor immunity. *Oncimmunology* 2016; **5**: e1085146.
61. Good-Jacobson KL, Szumilas CG, Chen L, Sharpe AH, Tomayko MM, Shlomchik MJ. PD-1 regulates germinal center B cell survival and the formation and affinity of long-lived plasma cells. *Nat Immunol* 2010; **11**: 535–542.
62. Ren Z, Peng H, Fu Y-X. PD-1 shapes B cells as evildoers in the tumor microenvironment. *Cancer Discov* 2016; **6**: 477–478.

63. Cubas RA, Mudd JC, Savoye A-L, *et al.* Inadequate T follicular cell help impairs B cell immunity during HIV infection. *Nat Med* 2013; **19**: 494–499.
64. Hiramatsu Y, Suto A, Kashiwakuma D, *et al.* c-Maf activates the promoter and enhancer of the IL-21 gene, and TGF-beta inhibits c-Maf-induced IL-21 production in CD4<sup>+</sup> T cells. *J Leukoc Biol* 2010; **87**: 703–712.
65. Liu XK, Zhao HM, Wang HY, *et al.* Regulatory effect of Sishen Pill on Tfh cells in mice with experimental colitis. *Front Physiol* 2020; **11**: e 589.
66. Dyck L, Mills KHG. Immune checkpoints and their inhibition in cancer and infectious diseases. *Eur J Immunol* 2017; **47**: 765–779.
67. Schaut RG, Lamb IM, Toepp AJ, *et al.* Regulatory IgD<sup>hi</sup> B Cells suppress T cell function via IL-10 and PD-L1 during progressive visceral Leishmaniasis. *J Immunol* 2016; **196**: 4100–4109.
68. Robilotti EV, Babady NE, Mead PA, *et al.* Determinants of COVID-19 disease severity in patients with cancer. *Nat Med* 2020; **26**: 1218–1223.
69. Taylor G. Animal models of respiratory syncytial virus infection. *Vaccine* 2017; **35**: 469–480.
70. Zielinska E, Liu D, Wu H-Y, Quiroz J, Rappaport R, Yang D-P. Development of an improved microneutralization assay for respiratory syncytial virus by automated plaque counting using imaging analysis. *Virology* 2005; **2**: 84.
71. Pedrazza L, Cubillos-Rojas M, De Mesquita FC, *et al.* Mesenchymal stem cells decrease lung inflammation during sepsis, acting through inhibition of the MAPK pathway. *Stem Cell Res Ther* 2017; **8**: 289.

## SUPPORTING INFORMATION

Additional supporting information may be found online in the Supporting Information section at the end of the article.

© 2020 Australian and New Zealand Society for Immunology, Inc.